



## Research Article

## Dealing with the heat: Assessing heat stress in an Arctic seabird using 3D-printed thermal models

Fred Tremblay<sup>a,\*</sup>, Emily S. Choy<sup>b</sup>, David A. Fifield<sup>c</sup>, Glenn J. Tattersall<sup>d</sup>, François Vézina<sup>e</sup>, Ryan O'Connor<sup>e</sup>, Oliver P. Love<sup>f</sup>, Grant H. Gilchrist<sup>c</sup>, Kyle H. Elliott<sup>a</sup>

<sup>a</sup> Department of Natural Resource Sciences, McGill University, Canada

<sup>b</sup> Department of Biology, McMaster University, Canada

<sup>c</sup> Wildlife Research Division, Environment and Climate Change Canada, Canada

<sup>d</sup> Department of Biological Sciences, Brock University, Canada

<sup>e</sup> Département de biologie, chimie et géographie, Université du Québec à Rimouski, Canada

<sup>f</sup> Department of Integrative Biology, University of Windsor, Canada



## ARTICLE INFO

Edited by Michael Hedrick

## Keywords:

Biophysical model

*Uria lomvia*

Thick-billed-murre

Evaporative water loss

Operative temperature

## ABSTRACT

The Arctic is warming at four times the global average rate and most studies have focused on the indirect (e.g., changes in food web) rather than the direct effects of climate change. However, as Arctic animals often have low capacity to dissipate heat, the direct effect of warming could impact them significantly (heat stress). To study heat stress, biophysical models have been used in many species to estimate operative temperature ( $T_e$ , integrated temperature of the thermal environment experienced by an individual). Here, we developed biophysical models of an Arctic seabird, the thick-billed murre (*Uria lomvia*). We demonstrated that 3D-printed painted models perform similarly to the more traditionally used feather-covered models. We deployed our models on Coats Island, Nunavut, Canada to study heat stress, which occurs in murrens when operative temperature is above 21.2 °C (the temperature at which evaporative water loss (EWL) rates increase to maintain a constant body temperatures). Murre operative temperatures ranged from 5.5 °C to 46.5 °C despite ambient temperatures never exceeding 24.7 °C (range: 3.4–24.7 °C), and murrens experienced heat stress on 61 % of the days during the breeding season (range: 24–85 %). Using known equations of EWL as a function of temperature, we estimated that murrens lost 3.79 % to 4.61 % of their body mass in water daily. Our study confirms the physiological challenges faced by Arctic seabirds during the breeding season, while also demonstrating the value of biophysical models as non-invasive tools to study the effects of heat stress on seabirds.

## 1. Introduction

The Arctic is warming at four times the global average rate (Chylek et al., 2022; Rantanen et al., 2022), affecting many basic ecological processes (Dobson et al., 2015; Post et al., 2009). With the projected increase in temperature, Arctic and sub-Arctic animals are experiencing negative effects because of indirect changes linked to climate change, such as changes in species interactions (Dey et al., 2017; Juhasz et al., 2020), and phenological mismatch (Clausen and Clausen, 2013)]. However, few studies have documented direct effects of climate change such as changes in physiological processes. Examples might include higher water loss, energy expenditure and/or heat dissipation as a direct

response of increasing temperature. These issues have been rarely studied, perhaps because Arctic temperatures are typically low and, consequently, it is thought that wildlife should be able to cope with such temperatures and not be exposed to heat stress in general (but see Choy et al., 2021; O'Connor et al., 2022).

Most Arctic animals are well adapted to withstand extreme cold temperatures either via behavioural adaptations (i.e., wintering under snow to insulate themselves), physiological adaptations (e.g., effective counter-current heat exchange), or physical adaptations to minimize heat loss (e.g., thick coats or dense plumage, adaptive coloring to absorb heat from light, or short limbs; Blix, 2016). For species that are adapted to withstand extreme cold temperatures, a warming environment might

\* Corresponding author at: Canadian Wildlife Service, Environment and Climate Change Canada, 351 Boul. Saint-Joseph, Gatineau, QC, Canada.

E-mail address: [frederique.tremblay@ec.gc.ca](mailto:frederique.tremblay@ec.gc.ca) (F. Tremblay).

@FredTremblay17 (F. Tremblay)

<https://doi.org/10.1016/j.cbpa.2025.111880>

Received 13 February 2025; Received in revised form 6 May 2025; Accepted 12 May 2025

Available online 18 May 2025

1095-6433/© 2025 The Authors. Published by Elsevier Inc. This is an open access article under the CC BY license (<http://creativecommons.org/licenses/by/4.0/>).

challenge their survival due to their limited capacity to dissipate heat (Oswald and Arnold, 2012). Thus, despite the limited work on direct effects, heat stress has the potential to affect Arctic wildlife at a much faster rate than indirect effects, leading to expected reductions in breeding success (O'Connor et al., 2022) and mortality events (Gaston et al., 2002; McKechnie and Wolf, 2010).

In seabirds, the breeding season typically corresponds with higher ambient temperatures, especially in Polar Regions where birds are exposed to continuous or near-continuous sunlight and must remain at their nest for long periods caring for young (Love et al., 2010). Birds are homeothermic endotherms and must attempt to maintain a constant body temperature. They use an array of strategies to retain or dissipate heat since metabolic costs increase if they cannot remain in their thermoneutral zone, where metabolic costs of thermoregulation are otherwise minimal (Scholander et al., 1950). Because an endotherm's energy output can be limited by their capacity to dissipate heat (e.g., heat dissipation limit theory; Speakman and Król, 2010), effective evaporative heat dissipation is essential for tolerating high ambient temperatures in a warming environment, since non-evaporative mechanisms are diminished (O'Connor et al., 2024). Yet, the capacity to dissipate heat can result in trade-offs between thermoregulation and other breeding functions, and therefore can result in costs to reproduction (Conradie et al., 2019; Oswald and Arnold, 2012; Cook et al., 2020; Choy et al., 2021, but see Beaman et al., 2024; Olin et al., 2023). While studies on the capacity of Arctic seabirds to tolerate extreme cold are available (Scholander et al., 1950; Le Pogam et al., 2020; Blix, 2016), very limited information is available on their capacity to tolerate heat (Oswald and Arnold, 2012).

The thick-billed murre (*Uria lomvia*; hereafter: murre) is a widespread Arctic seabird that nests on sun-exposed cliffs where both adults care for their offspring. During the day, an individual will incubate the nest for up to 12h until its mate returns from foraging and switch duties with its partner by incubating during the night (Gaston and Hipfner, 2020). On Coats Island, Nunavut, Canada, a well-studied murre colony (Patterson et al., 2024), males typically incubate during the day while females incubate at night (Patterson et al., 2024). While incubating, a murre must remain on its nest to protect their single egg from predation (Gilchrist et al. 1998), as well as prevent it from being accidentally dislodged by other murrens (Gaston and Hipfner, 2020). Incubating their eggs for extended periods can be challenging on hot days as incubating murrens cannot leave their nesting ledge to cool off in the sea without risking the loss of their single egg or chick (Choy et al., 2021). Moreover, as males incubate during the day on Coats Island, they are likely to be exposed to heat stress much more frequently than females.

Murrens are diving seabirds that experience an array of thermal conditions including the heat generated from direct solar radiation on their black plumage while they incubate, to sub-zero temperatures of the waters in which they forage. Murrens have the lowest maximum evaporative cooling efficiency ever measured in birds, presumably reflecting their adaptation to extreme cold temperatures (Choy et al., 2021). However, murrens experience heat stress (hereby defined as the inflection point that denotes the minimum temperature after which a significant increase in evaporative water loss is observed) at ambient temperatures as low as 21.2 °C. At ambient temperatures of 21.2 °C and above, their rate of evaporative water loss (EWL) increases significantly, with higher evaporative water loss rates occurring in smaller individuals (body mass ranging from 906 g–1079 g; Choy et al., 2021). In the field, mortality of incubating murrens has been reported on days with ambient temperatures as low as 22 °C due to acute dehydration (Gaston et al., 2002). These results highlight the need for further research on climate change-induced heat stress that murrens may experience at a colony during the breeding season. This is especially relevant as heat stress could disproportionately affect certain demographic groups, namely males as they attend the nest during the day on Coats Island and older individuals that are expected to be more prone to acute dehydration (Gaston and Elliott, 2013).

The operative temperature ( $T_o$ ) refers to the integrated temperature of an environment as experienced by an individual in that given environment. Operative temperature often differs from ambient temperature, as an individual's perception of its thermal environment results from a combination of its morphology (e.g., shape, size, colour) and the influence of its microclimate on heat exchange pathways (Bakken and Gates, 1975; Bakken, 1976; Bakken and Angilletta Jr, 2014). These pathways include convection (e.g., the effect of wind speed), conduction (e.g., heat exchange with the ground substrate) and radiation (e.g., reflection from surrounding surfaces, sun exposure) (Dzialowski, 2005). As such, animals that are exposed to direct sun, such as cliff-nesting seabirds, often experience operative temperatures in their thermal environment that are much higher than ambient temperature (Schreiber and Burger, 2001).

To estimate operative temperature, biophysical models have been used in an array of ectotherms (Bakken and Gates, 1975; Grant and Dunham, 1988; Hertz, 1992), and a few endotherms (Sears et al., 2006; O'Connor et al., 2018; O'Connor et al., 2022). When designed properly, biophysical models yield a single estimate of temperature that considers the various pathways of heat exchange: convection, conduction, and radiation (Bakken, 1976). Thus, biophysical models aim to reproduce a given specimen as closely as possible in terms of size, shape, and colouration (i.e., solar reflectance), with the intent to generate the thermal conditions similar to those experienced by the species in their environment (Bakken and Gates, 1975; Bakken, 1976; Shine and Kearney, 2001).

Under controlled laboratory conditions (i.e., where ambient temperature = operative temperature) murrens experience heat stress despite air temperatures being as low as 21.2 °C (Choy et al., 2021). Concomitantly, Gaston et al. (2002) found that the black plumage on the backs of murrens could reach temperatures as high as 47 °C when exposed to full sun with air temperatures as low as 22 °C, highlighting the importance of studying heat stress experienced by murrens under real nesting conditions. Here, we use biophysical models to assess incidences of potential heat stress in murrens which we define as operative temperatures beyond their EWL inflection point. We estimate EWL throughout the day, at different colony locations, and nest microhabitats. We predict that 1) biophysical models can be used to accurately estimate operative temperature of murrens, and 2) that murrens do experience heat stress regularly, especially during the day when males are most likely to be incubating. Likewise, we predict that murrens' EWL estimated using operative water loss will be higher than when estimated from ambient temperature.

## 2. Methods

### 2.1. Model development

We designed biophysical models for 3-D printing to assess the operative temperature of breeding murrens. As a first step, we completed material testing to evaluate which material and wall thickness of the hollow models was most appropriate to validate the design of our biophysical model (see Supplementary Material 1 for details on material testing). Following this, we 3D printed our models in polyethylene terephthalate glycol (hereafter PETG; black 1.75 mm PETG filaments from DURAMIC 3D, product # 612677937130) with a wall thickness of 3.2 mm.

Using deceased murrens, we measured the spectral reflectance of both the white plumage (ventral plumage) and black plumage (dorsal plumage, head feathers, and wing coverts) using a hand-held photo spectrometer (Ocean Optics™ Red Tide USB 650) connected to a light source (tungsten-halogen, Ocean Optics™ LS-1). Murrens were collected by hunters as part of a subsistence hunt in Newfoundland, Canada (provided by ECCC). We painted the biophysical models to approximate murre colouration as accurately as possible, using Benjamin Moore outdoor paint in colours HC-190 and AF-195, given that their light

reflectance values (Light reflectance value = 2.48 % and light reflectance value = 52.76 % respectively) matched the black and the white feathers' reflectance ( $r = 1.52 \pm 1.24$  % and  $r = 47.49 \pm 9.60$  % respectively).

We also fitted a subset of models with murre skin and feathers to compare temperature readings against the painted models. The murre skin and feathers covered the 3D printed biophysical models completely except the bill, legs and base (Fig. 1). To record operative temperature, we fixed an iButton (models DL1925L-F5 and DL1921G-F5) in the center of the body cavity of each biophysical model and recorded temperature at an interval of 10 min with a precision of 0.5 °C. We fixed the iButtons by gently gluing them to a long and narrow skewer inserted from a hole at the base of the model. This way, it allowed the iButton to float in the center of the body cavity without touching any wall. The hole at the base of the cavity was completely sealed using a rubber plug on which the skewer was attached.

## 2.2. Field validation of spectral reflectance

To validate the use of the painted model against the feathered model (considered as being the "truer" model), we deployed both in the field on Coats Island (62°35'N 082°45'W), Nunavut, between July 10th and August 7th, 2022, a colony that supports 30,000 breeding pairs of murres (Fig. 2). We simultaneously recorded infrared images of the back of the painted model, the feathered model and live breeding murres to evaluate how their back temperatures compared under the same conditions. We predicted that if the reflectance of the model colour was well matched to the real feathers of murres, there would be no difference in the temperature measured from their back. We captured infrared images of breeding murres and models using a FLIR T1030sc camera and a telephoto lens with a focal length of 83.4 mm (12°; IFOV of 0.20 mrad). We captured images regularly, but on an opportunistic basis (every two to five days from 12 July to 27 July 2022), to intentionally account for the effects of environmental conditions on back temperature. Each time we captured an image, we recorded ambient temperature (°C), and relative humidity (%) using a Kestrel 0830 portable weather station (Kestrel Meter; Boothwyn, PA) within 10 m of the experimental and real birds. We also estimated the sky reflected temperature (°C) by capturing a thermal image of a crumpled ball of aluminium foil lying on the colony ground facing the sky (Usamentiaga et al., 2014). We estimated the distance (m) between the camera's lens and the object of the photo based on the assumption that murres are 30 cm high. To ensure reproducibility, all distances were estimated by the same person.

We analyzed all images using ThermImageJ functions (Tattersall, 2019) in FIJI (Schindelin et al., 2012), which are based on the same algorithms used in FLIR software. We compared the back temperature of feathered and painted models to the back temperature of a real murre ( $n = 44$  images). We extracted mean back temperature, where the back area is defined as the area of black feathers starting at the base of the neck to the base of the tail, and delimited on both sides by the wings,



Fig. 1. Thick-billed murre models, with the feathered models in the front on the left and the painted models in the back row.

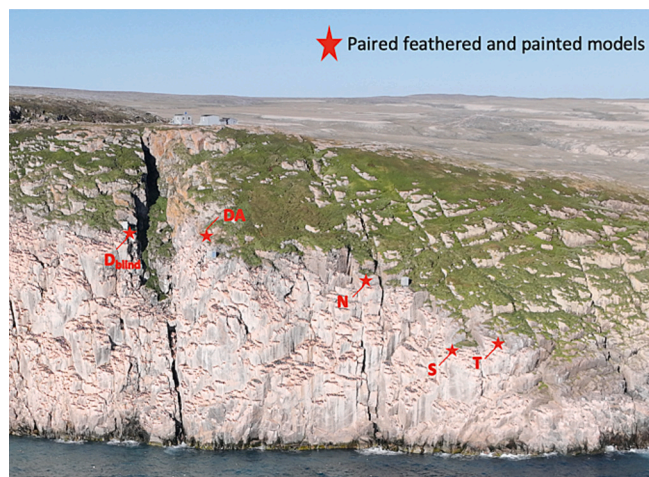


Fig. 2. Biophysical models of thick-billed murres deployed in colony on Coats Island, Nunavut, Canada ( $n = 5$  painted and 5 feathered models). Plot names are indicated by the letters linked to the stars, where red stars denote sites where we deployed both a painted and a feathered model. (For interpretation of the references to colour in this figure legend, the reader is referred to the web version of this article.)

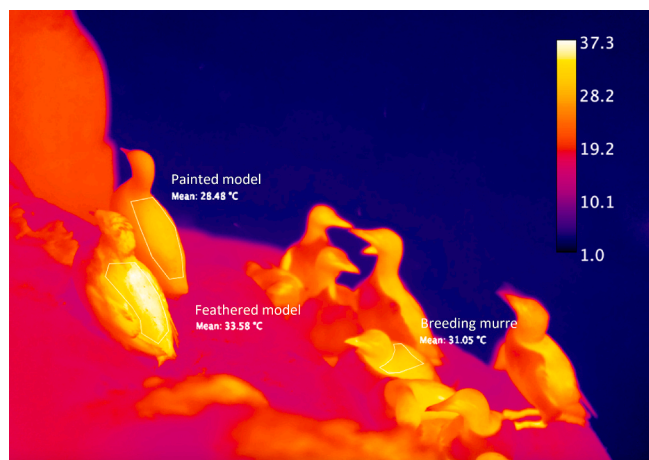


Fig. 3. Example thermal image of biophysical models and live thick-billed murres in the breeding colony at Coats Island, Nunavut, Canada. For each model and murres where at least 1/3 of the back is visible, the back area is indicated by the white perimeter with associated mean back temperature to the right.

excluding upper wing coverts (Fig. 3). As the painted models do not have strict body feathers/wing delimitation, we estimated the delimitation while ensuring that only the black area was included in the image sampling.

To compare the performance of the biophysical models to the real murre's plumage and allow for comparison between the biophysical model types, we modelled back temperature using a mixed effect model and the *lme4* package (Watson and Francis, 2015) in R 4.2.1 (R Core Team, 2022). We used back temperature ( $T_{back}$ ) as the response variable and added biophysical model type (real murre, painted or feathered), cloud cover (in %), ambient temperature ( $T_a$ ) and sky reflected temperature ( $T_r$ ) as fixed effects in interaction with cloud cover, with colony location (plot) as a random effect (see Eq. (1)).

$$T_{back} = T_a^* \text{Cloud Cover} + T_r^* \text{Cloud Cover} + \text{Model Type} + (1|\text{Plot}) \quad (1)$$

### 2.3. Field study design

To investigate incidences of heat stress in breeding murres, we estimated the operative temperatures and rates of EWL experienced by murres breeding on Coats Island. We estimated operative temperature using the biophysical models of murres described above and fitted them with iButtons to record temperature at five locations (Fig. 2), representing the range of environments occupied by breeding murres near the top (vertically) of the colony where heat stress is expected to be greatest (Gaston and Elliott, 2013). We conducted all statistical analyses using R 4.2.1 (R Core Team, 2022).

### 2.4. Measurements of operative temperature

We obtained estimates of operative temperature from the iButton fixed internally within each biophysical model. We did not obtain data from 14 July to 18 July at one of our colony locations (D blind) as the models were blown into the sea during a storm. Additionally, we did not obtain data from 26 July to 31 July at two colony locations (D blind and T) and from 1 July to 7 July at one colony location (S) due to iButton malfunction (Fig. 2).

To ensure that the painted and feathered models yielded comparable estimates of operative temperature, we compared their estimates of operative temperature at the five colony locations. We first conducted a two-tailed Welch *t*-test to test for statistical differences between the models. We then corrected the operative temperature values from the painted model using a linear regression to allow for comparison between the painted and the feathered models' operative temperature:

$$T_{e-feather} \sim T_{e-paint} * 1.02 + 0.57 \quad (2)$$

where  $T_{e-paint}$  and  $T_{e-feather}$  correspond to the operative temperatures recorded by the painted and feathered models respectively. All operative temperatures reported in results reflect the corrected operative temperature.

### 2.5. Evaporative water loss

To assess the risk of mortality from heat, we compared the predicted rate of EWL in murres when calculated using operative temperature versus ambient temperature. To estimate EWL (in  $g\ h^{-1}$ ) in murres at the Coats Island colony, we used equations of EWL as a function of temperature (Eqs. (3), (4)) published by Choy et al. (2021),

$$EWL = T^* 0.14 + Mb^* 0.00363 - (T^* Mb^* 0.000126) - 2.4; \text{ if } T > 21.2^\circ C \quad (3)$$

$$EWL = Mb^* 0.0015 + 0.0876; \text{ if } T < 21.2^\circ C \quad (4)$$

where  $M_b$  corresponds to body mass (in grams) and  $T$  corresponds to

either operative or ambient temperature (in  $^\circ C$ ). For operative temperature and ambient temperature above or equal to the inflection point of  $21.2^\circ C$ , we used Eq. (3) and used Eq. (4) for all other values of operative temperature ( $< 21.2^\circ C$ ). As Choy et al. (2021) reported a significant difference in rate of EWL based on masses below and above 900 g, we calculated EWL for a theoretical murre of 800 g, 900 g and 1000 g to capture a wide range of body masses. We also calculated EWL as a proportion of body mass (in %) loss per day murres of 800 g and 1000 g (Gaston and Hipfner, 2020) based on the hourly rate of EWL, over a 24 h period starting at midnight.

While Choy et al. (2021) report an inflection point at  $21.2^\circ C$  for murres, they also noted that one bird visually had a lower EWL than others. Though not a significant outlier, when that bird was removed, the EWL inflection point shifted to  $24.5^\circ C$ . As such, we also calculated EWL using the equations provided by Dr. Choy via personal communication (2025) for an inflection point  $24.5^\circ C$  where:

$$EWL = T^* 0.12 + Mb^* 0.0031 - (T^* Mb^* 0.0001076) - 1.778; \text{ if } T > 24.5^\circ C \quad (5)$$

$$EWL = Mb^* 0.00147 + 0.1302; \text{ if } T < 24.5^\circ C \quad (6)$$

To compare EWL estimated using the two different inflection points, we conducted a simple paired *t*-test.

## 3. Results

### 3.1. Field validation of spectral reflectance

We confirmed that the colour used on the painted models was appropriate, as the reflectance measured did not differ from that of the feathered model ( $t_{105} = -1.45, p = 0.15$ ; Fig. 4) or of the real, incubating murres ( $t_{105} = -0.52, p = 0.61$ , Fig. 4). Environmental conditions, such as cloud cover and ambient temperature, were the main predictors of back temperatures as predicted (see Supplementary Materials 2 for full model output).

### 3.2. Operative temperature

We recorded a total of 32,780 measurements of operative

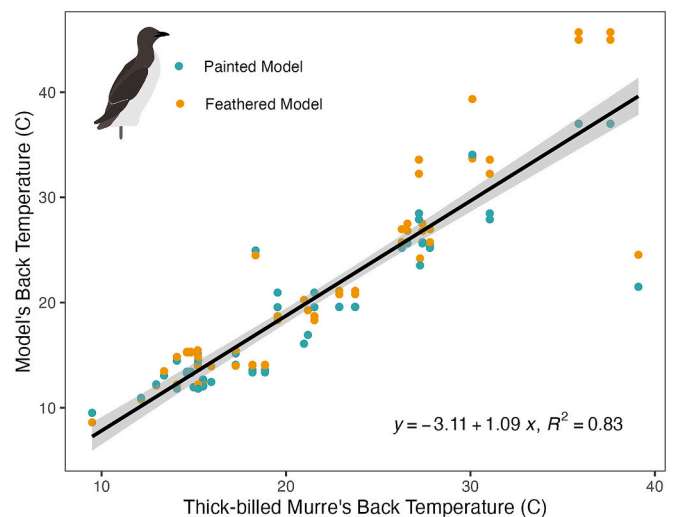


Fig. 4. Back temperatures of biophysical models (blue = painted models and tan = feathered models) compared to simultaneous murres' back temperature measurements showing that the coloration of the 3D printed biophysical models (both painted and feathered) are appropriately mimicking the spectral reflectance of real murres. (For interpretation of the references to colour in this figure legend, the reader is referred to the web version of this article.)

temperature between 10 July and 7 August 2022 among five different colony locations (Fig. 6). Operative temperature ranged between 5.5 °C and 46.5 °C, despite ambient temperature never exceeding 24.7 °C (range: 3.4–24.7 °C). Operative temperature averaged  $16.1 \pm 7.1$  °C during the day, and  $9.9 \pm 2.0$  °C at night (Table 1, but also see Supplementary Material 2). Assuming murres experience heat stress at operative temperatures above or equal to 21.2 °C (Choy et al., 2021), we estimated that murres experienced heat stress on average 61 % of the days that we recorded operative temperature, but that exposure to heat stress varied among colony locations ranging from 24 % to 86 % (Table 1). Diurnal operative temperature varied with colony location, with models deployed at D blind never getting warmer than 29.5 °C, while all other colony locations recorded temperatures above 40 °C, with a maximum of 46.5 °C recorded at DA (Table 1, Fig. 6).

### 3.3. Estimates of evaporative water loss

#### a. Using 21.2°C as inflection point

Average daily peak in EWL rate, using an inflection point of 21.2 °C, ( $\text{g h}^{-1}$ ) ranged between  $1.32 \pm 0.08$   $\text{g h}^{-1}$  and  $1.65 \pm 0.06$   $\text{g h}^{-1}$  (Table 2) when calculated using operative temperature. Daily EWL (% of  $M_b$ ) calculated from operative temperature averaged  $4.00 \pm 0.17$  % of body mass per day for a small murre ( $M_b = 800$  g) and  $3.82 \pm 0.03$  % of body mass per day for a larger murre ( $M_b = 1000$  g; Table 2). Daily EWL varied among different sites, where spatial variation in EWL was amplified in individuals with a lower body mass (Table 2). Mean daily EWL across sites ranged from 3.88 to 4.07 % of body mass for small individuals, whereas daily EWL only ranged from 3.80 to 3.83 % of body mass for larger individuals (Table 2).

Because operative temperatures often exceeded 21.2 °C while ambient temperatures stayed below that threshold, the mean evaporative water loss (EWL) estimated using operative temperature (colony mean range: 1.29–2.18  $\text{g h}^{-1}$ ) was equal to or higher than the estimates based on ambient temperature (range: 1.29–1.44  $\text{g h}^{-1}$ ; Fig. 7–8). However, the extent of the difference between EWL estimates based on ambient versus operative temperature varied across sites (Table 2). The difference between EWL calculated from ambient temperature versus operative temperature was significantly accentuated in individuals with a lower body mass (Table 2, Fig. 8).

#### b. Using 24.5 °C as inflection point

Changing the inflection point to 24.5 °C to estimate EWL resulted in an increase of 0.04 % in daily body mass loss across all weight categories ( $p < 0.001$  for a 880 g, 900 g and 1000 g bird).

## 4. Discussion

Using measurements of operative temperature collected from biophysical models of thick-billed murres deployed at an Arctic seabird

**Table 1**

Minimum, maximum and mean operative temperature estimated from biophysical models deployed in various colony locations, and predicted percentage of days murres experienced heat stress. Heat stress is defined here as the temperature experienced by murres beyond their evaporative water loss inflection point ( $> 21.2$  °C; Choy et al., 2021).

Plot	n (# of measurements)	Min $T_e$ (°C)		Max $T_e$ (°C)		Mean $T_e \pm$ SD (°C)		$T_e > 21.2$ °C (% Days)
		Day	Night	Day	Night	Day	Night	
D blind	5038	5.5	6.0	29.5	15.4	$13.1 \pm 4.3$	$9.25 \pm 1.8$	24
DA	7934	5.5	6.0	46.5	17.0	$17.2 \pm 8.2$	$10.1 \pm 2.1$	72
N	8012	5.5	6.0	42.0	17.0	$14.9 \pm 6.0$	$10.0 \pm 2.0$	59
S	5978	6.0	6.5	42.4	17.5	$17.9 \pm 7.7$	$10.5 \pm 2.1$	86
T	5818	5.5	6.0	40.0	15.4	$16.5 \pm 7.1$	$9.7 \pm 1.7$	65
Colony Avg	32,780	5.5	6.0	46.5	17.5	$16.1 \pm 7.1$	$9.9 \pm 2.0$	61

**Table 2**

Average daily peak in EWL rate ( $\text{g h}^{-1}$ ), daily EWL (%  $M_b$ ), and mean difference in average daily evaporative water loss calculated using  $T_e$  at different colony location compared to daily EWL calculated from  $T_a$ .

Plot	N	Maximum EWL ( $\text{g h}^{-1}$ )		Avg Daily Maximum EWL $\pm$ SD ( $\text{g h}^{-1}$ )		Avg Daily Maximum EWL $\pm$ SD ( $\text{g h}^{-1}$ )	
		$M_b = 800$ g	$M_b = 1000$ g	$M_b = 800$ g	$M_b = 1000$ g	$M_b = 800$ g	$M_b = 1000$ g
D blind	422	1.62	1.63	$1.32 \pm 0.08$	$1.59 \pm 0.01$	$1.32 \pm 0.08$	$1.59 \pm 0.01$
DA	662	2.18	1.83	$1.59 \pm 0.27$	$1.64 \pm 0.07$	$1.59 \pm 0.27$	$1.64 \pm 0.07$
N	668	1.98	1.76	$1.44 \pm 0.18$	$1.61 \pm 0.04$	$1.44 \pm 0.18$	$1.61 \pm 0.04$
S	499	2.03	1.77	$1.63 \pm 0.22$	$1.65 \pm 0.06$	$1.63 \pm 0.22$	$1.65 \pm 0.06$
T	483	1.95	1.75	$1.52 \pm 0.21$	$1.62 \pm 0.05$	$1.52 \pm 0.21$	$1.62 \pm 0.05$
Colony Avg ( $T_e$ )	2737	2.18	1.83	$1.51 \pm 0.23$	$1.62 \pm 0.06$	$1.51 \pm 0.23$	$1.62 \pm 0.06$
Colony Avg ( $T_a$ )	791	1.44	1.44	$1.30 \pm 0.03$	$1.29 \pm 0.03$	$1.30 \pm 0.03$	$1.29 \pm 0.03$

colony, we investigated heat stress experienced by murres while on cliff ledges within a breeding colony. Prior to deployment, we validated the use of our 3D printed models to measure operative temperature in murres, using both in vitro tests to validate the material properties of the 3D printed models (Supplementary Material 1) and field tests to validate the spectral reflectance of the models compared to real murres (Fig. 5). Collectively, this laid the path for more affordable and easily produced biophysical models for large birds.

3D-printing offers an innovative and simpler method for producing biophysical models compared to traditional techniques (e.g., copper molding). The validation of painted models, rather than using fitted skins, further simplifies the process. As shown in the results, the operative temperature recorded by painted models differs from that of feathered models, but in a predictable manner. While we account for solar radiation by ensuring that the paint colour matches the spectral reflectance of the plumage, the effect of wind may not be captured as accurately due to the painted model's smoother surface, likely explaining the observed variation. In this regard, feathered biophysical models are likely better suited to representing the effects of wind on the operative temperature of live murres. Nonetheless, once corrected for this slight variation, we believe painted models remain highly valuable and closely approximate the conditions experienced by murres, enabling meaningful comparisons.

As expected, murres experienced generally higher temperatures than previously appreciated, based on measurements of operative compared to ambient temperature (Fig. 7). Under experimental conditions, where

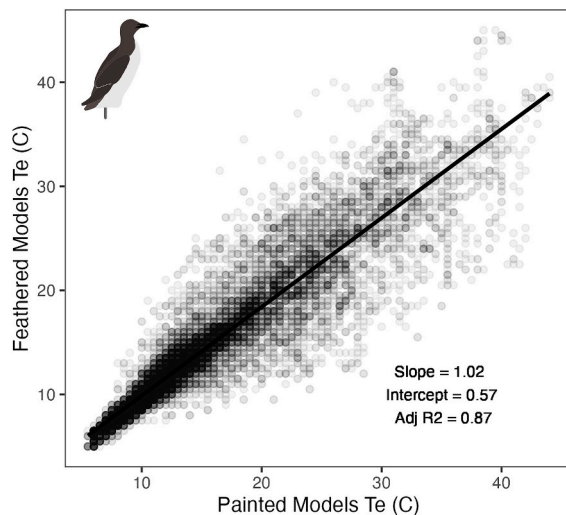


**Fig. 5.** Raw operative temperature from painted biophysical models compared to feathered biophysical models of thick-billed murres showing comparable temperature readings. Operative temperature was measured using iButtons fitted inside the body cavity of the models.

heat exchange from conduction, convection, and radiation can be controlled for or omitted completely, ambient temperature equals operative temperature (Shine and Kearney, 2001). However, in the field, birds are exposed to heat gain by radiation and heat loss by conduction and convection (O'Connor et al., 2018; O'Connor et al., 2022; Shine and Kearney, 2001). Cliff nesting seabirds such as murres are exposed to long periods of direct radiation from the sun, with no access to thermal refuge or water while attending their nest (Gaston and Hipfner, 2020). Although the ocean might offer a way to cool down when conditions are too warm, birds leaving their nests unattended risk losing their only egg (Gaston et al., 2002).

In conditions such as when solar radiation is high or wind is low or absent, operative temperature can surpass ambient temperature, and therefore, ambient temperature underestimates the extent of heat stress experienced by Arctic animals. While non-cliff-nesting species may have greater capacity to behaviourally adapt to warming temperatures, cliff-nesting species are more restricted in their ability to avoid heat. For example, gull species such as Glaucous Gulls nest in a variety of habitats and have highly mobile young, making it possible for them to move with their chicks to shaded areas to escape the heat. Similarly, Arctic Foxes that are often seen around the colony have the ability to avoid the heat by avoiding the sun and hiding in cooler crevasses, allowing them to better cope with high solar radiation and heat. In contrast, incubating murres are constrained to their breeding ledges where moving around or even turning in place on their ledge to hide their black back from absorbing the heat is not possible, limiting their ability to avoid elevated temperatures. Heat stress therefore is often the result of a trade-off to ensure successful breeding (Olin et al., 2023). In combination with recent work (O'Connor et al., 2022), our study highlights the importance of estimating operative temperatures of Arctic species in the field to more accurately understand the environmental conditions in which endotherms experience heat stress.

Exposure to heat stress in murres varied with time of day at the colony. Murres experienced the highest rates of estimated evaporative water loss during the day and the lowest rates at night. As males attend the nest during the day and females at night at this colony (Elliott et al., 2010), the direct effects of heat stress are likely to impact males more strongly over time than females. As the sex attending the nest during the day changes is colony-specific in murres, this behavioural plasticity might become an advantage to adapt to warming climate over other cliff-nesting species that do not exhibit such plasticity. Additionally, it

has been shown that older murres are less likely to abandon the nest even when under acute dehydration, resulting in disproportionate mortality of older murres in acute events at the colony (Gaston and Elliott, 2013). As the male exclusively cares for the chick at sea for ~37 days after departing the nest, the loss of older males may then have a disproportionate impact on demography and eventual fledging success (Gaston and Elliott, 2013).

We defined heat stress as incidences when murres experience operative temperature above 21.2 °C based on findings from Choy et al. (2021). However, we also estimated EWL using an alternative inflection point of 24.5 °C as Choy et al. (2021) noted that one individual, though not statistically an outlier, was driving down the inflection point. While the difference in % of body mass loss was significantly different when using an inflection point of 24.5 °C, we would argue that an increase of 0.04 % is not biologically significant, and therefore our results indicate that murres would still experience heat stress regularly (Fig. 6–7). While our study provides a broad and likely oversimplified view of heat-stress, it sheds light on a key point: using ambient temperature to evaluate heat stress can lead to a gross underestimation of reality. Our study clearly highlights the need of using operative temperature, rather than ambient temperature, when evaluating the direct effects of weather events and climate change on wildlife. We suggest that using operative temperature is therefore imperative in heat stress studies as it provides a better mean of understanding the true conditions experienced by murres. A similar study by O'Connor et al. (2022) using biophysical models to study heat stress in Snow bunting, a small arctic passerine, also drew similar conclusions.

Endotherms can only tolerate evaporative water loss up to a critical threshold before fatal dehydration occurs. For desert birds, this lethal dehydration limit has been estimated at approximately 15 % of body mass (Albright et al., 2017; Conradie et al., 2019), despite their adaptations to low water availability. Although the lethal dehydration limit for murres is currently unknown, and observed dehydration rates in murres were well below this threshold (maximum of 4.07 % of body mass), the potential sub-lethal effects of dehydration should not be overlooked. For instance, Conradie et al. (2019) projected significant conservation impacts on arid-zone African birds with evaporative water loss as low as ~4 % of body mass. Similarly, in bank cormorants (*Phalacrocorax neglectus*), heat-induced behavioural adjustments at the nest expose eggs and chicks to sub-optimal conditions and heightened predation risk, ultimately reducing breeding success (Cook et al., 2020). Given these findings, it is critical to investigate potential sub-lethal effects of dehydration in murres, which could include altered behavior, reduced breeding success, or other physiological consequences.

While we reported daily EWL estimates that accounted only for ~1/3 of the lethal dehydration limit, we did not account for other sources of dehydration. In murres, mortality at the colony has been observed on five instances under warm (>18 °C) conditions coupled with high mosquito density (Gaston et al., 2002; Gaston and Elliott, 2013). Necropsies of the deceased individuals reported acute dehydration as the cause of death, likely due to the combined effects of heat stress and mosquito parasitism (Gaston and Elliott, 2013; Gaston et al., 2002). In a year of comparatively cool conditions (no mortality observed), murres sitting on the nest on an exposed site lost up to 4.07 % of their body mass in water on a hot day (Table 2). When coupled with water loss from mosquitoes (Gaston and Elliott, 2013), and considering that fact that mortality can occur when birds lose 15 % of their body mass due to dehydration (Albright et al., 2017; Conradie et al., 2019), this could explain the high mortality previously reported even in warm, yet not extreme, years (Gaston et al., 2002). While we did not observe mortality in the colony at temperatures as low as 22°C as observed by Gaston et al., (2002), we suspect that the effect of wind is likely also at play as it would increase convective evaporative cooling and limit the number of mosquitoes present at the colony. Indeed, murre mortality is generally limited to calm days (Gaston and Elliott, 2013; Gaston et al., 2002).

To conclude, our study highlights the physiological challenges faced

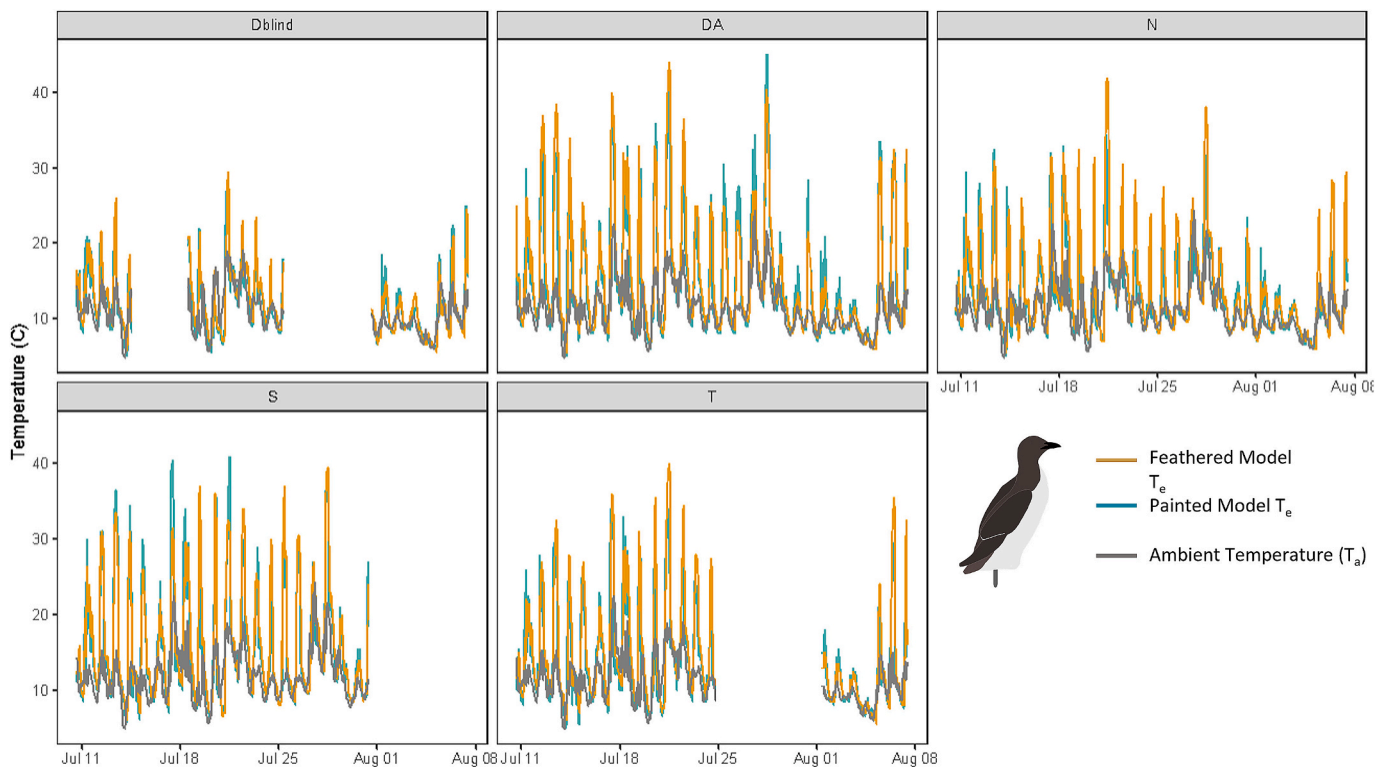


**Fig. 6.** Operative temperature ( $T_e$ ) from feathered models (tan) and painted models (blue) compared to ambient temperature (grey) over the length on the model deployment, starting on July 11th to August 8th, showing that operative temperature frequently exceeds ambient temperature, following a diurnal pattern. Each panel represents a different colony location. (For interpretation of the references to colour in this figure legend, the reader is referred to the web version of this article.)

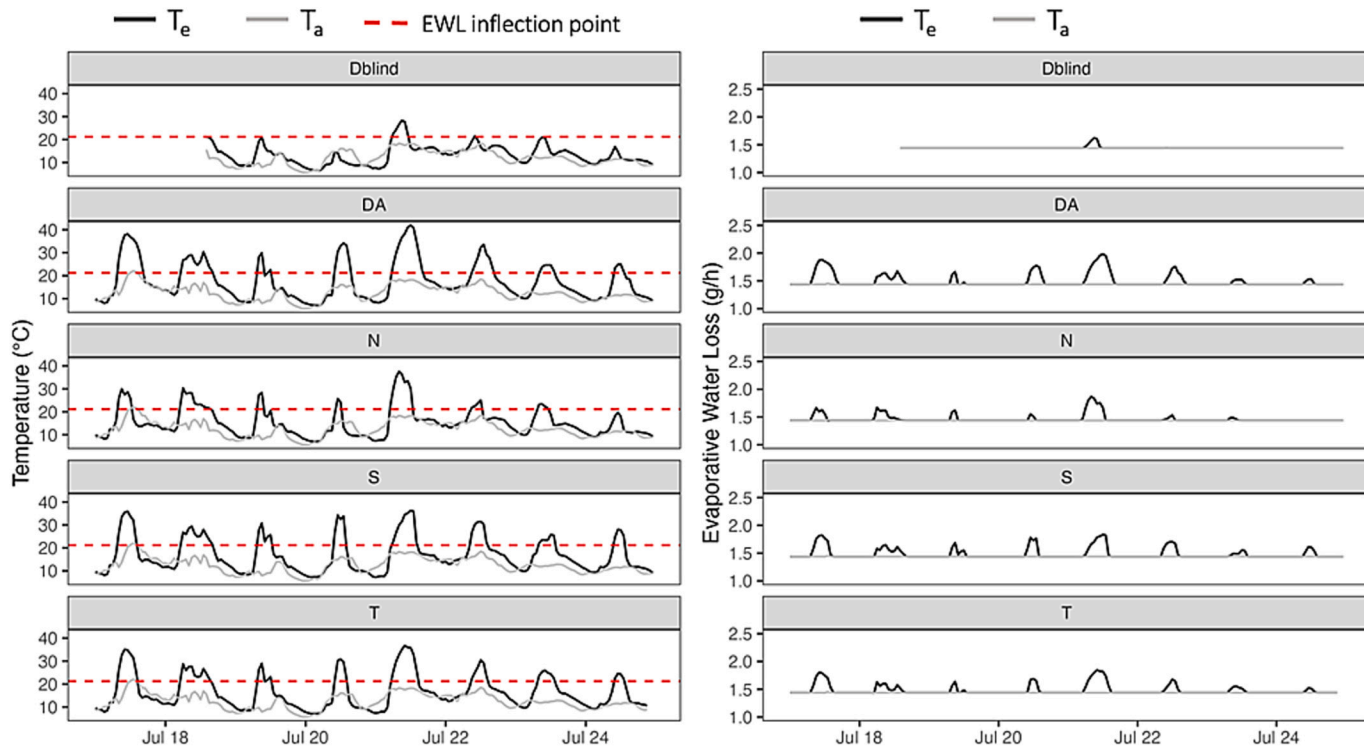


**Fig. 7.** Comparison of temperature and associated evaporative water loss for an averaged size murre of 900 g when using operative temperature ( $T_e$ ) vs ambient temperature ( $T_a$ ) at various colony locations showing that thick-billed murres frequently experience heat stress as operative temperature is regularly above the evaporative water loss inflection point (at 21.1 °C), even though ambient temperature remains below that point.

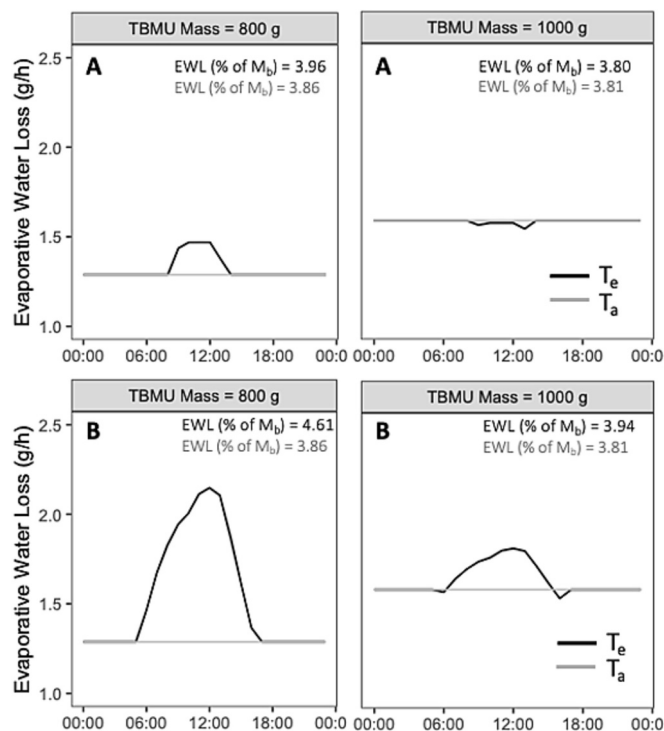


**Fig. 8.** Evaporative water loss (EWL; in  $\text{g h}^{-1}$ ) of thick-billed murres (TBMU) calculated using operative temperature ( $T_e$ ; black) and ambient temperature ( $T_a$ ; grey) on a day with **A**) low maximum operative temperature ( $T_e$  max =  $24.6\text{ }^\circ\text{C}$ ) and **B**) high operative temperature ( $T_e$  max =  $41.9\text{ }^\circ\text{C}$ ). Evaporative water loss is also reported as a percentage of body mass lost over the 24 h period.

by Arctic seabirds during the breeding season which are only expected to increase under climate change. Although indirect effects (changing prey base, increased predation, and parasitism) are known to impact murre demography, the role of direct heat stress in light of apparent declines of this species (Frederiksen et al., 2016) cannot be ignored. Understanding thermal physiology of wild birds and the factors affecting that, can shed light on the challenges that these individuals face as the climate warms. Despite the fact that we cannot control the increase in ambient temperature, we can consider the various paths of heat exchange that influence operative temperature to develop better conservation plans (i.e., tracking shifts in habitat preference within and among colonies, or perhaps preserving habitats that provide shade to act as thermal refuge (Elmore et al., 2017)). While more research on the direct effects of climate is needed, conservationists and policymakers can start addressing this issue by shifting conservation practices to incorporate the role of microhabitats in species protection, in addition to the already established focus on large conservation areas.

#### CRedit authorship contribution statement

**Fred Tremblay:** Writing – review & editing, Writing – original draft, Visualization, Methodology, Funding acquisition, Formal analysis, Data curation, Conceptualization. **Emily S. Choy:** Writing – review & editing, Validation, Supervision, Conceptualization. **David A. Fifield:** Writing – review & editing, Validation, Software, Resources, Methodology. **Glenn J. Tattersall:** Writing – review & editing, Validation, Software, Methodology. **François Vézina:** Writing – review & editing, Resources, Methodology. **Ryan O'Connor:** Writing – review & editing, Conceptualization. **Oliver P. Love:** Writing – review & editing, Conceptualization. **Grant H. Gilchrist:** Writing – review & editing, Resources. **Kyle H. Elliott:** Writing – review & editing, Supervision, Project administration, Funding acquisition, Conceptualization.

#### Declaration of competing interest

The authors declare the following financial interests/personal relationships which may be considered as potential competing interests:

Fred Tremblay reports financial support was provided by Natural Sciences and Engineering Research Council of Canada. Fred Tremblay reports financial support was provided by Northern Scientific Training Program. Fred Tremblay reports financial support was provided by Baffinland Iron Mines Corp. If there are other authors, they declare that they have no known competing financial interests or personal relationships that could have appeared to influence the work reported in this paper.

#### Acknowledgments

We gratefully acknowledge the NSERC-CRPD, Baffinland Iron Mines Corporation, and the Northern Scientific Training Program (NSTP) for their financial support of this research. We also extend our sincere thanks to Holly Hennin and Marianne Gousy-Leblanc, whose invaluable contributions made the fieldwork possible. Furthermore, we deeply appreciate Jade Legros for her invaluable advice and unwavering support throughout the manuscript preparation.

#### Appendix A. Supplementary data

Supplementary data to this article can be found online at <https://doi.org/10.1016/j.cbpa.2025.111880>.

#### Data availability

The cleaned data is publicly available and can be accessed following the link below. For more information please contact the corresponding author.

Link: <https://data.mendeley.com/datasets/6wz7jv7ncz/1>

#### References

- Albright, T.P., Mutiibwa, D., Gerson, A.R., Smith, E.K., Talbot, W.A., O'Neill, J.J., McKechnie, A.E., Wolf, B.O., 2017. Mapping evaporative water loss in desert passerines reveals an expanding threat of lethal dehydration. *Proc. Natl. Acad. Sci.* 114, 2283–2288.
- Bakken, G.S., 1976. A heat transfer analysis of animals: unifying concepts and the application of metabolism chamber data to field ecology. *J. Theor. Biol.* 60, 337–384.
- Bakken, G.S., Angilletta Jr., M.J., 2014. How to avoid errors when quantifying thermal environments. *Funct. Ecol.* 28 (1), 96–107.
- Bakken, G.S., Gates, D.M., 1975. Heat-transfer analysis of animals: Some implications for field ecology, physiology, and evolution. In: *Perspectives of Biophysical Ecology*. Springer Berlin Heidelberg, Berlin, Heidelberg, pp. 255–290.
- Beam, J.E., White, C.R., Clairbaux, M., Perret, S., Fort, J., Grémillet, D., 2024. Cold adaptation does not handicap warm tolerance in the most abundant Arctic seabird. *Proc. R. Soc. B* 291 (2023), 20231887.
- Blix, A.S., 2016. Adaptations to polar life in mammals and birds. *J. Exp. Biol.* 219 (8), 1093–1105.
- Choy, E.S., O'Connor, R.S., Gilchrist, H.G., Hargreaves, A.L., Love, O.P., Vézina, F., Elliott, K.H., 2021. Limited heat tolerance in a cold-adapted seabird: implications of a warming Arctic. *J. Exp. Biol.* 224, jeb242168.
- Chylek, P., Folland, C., Klett, J.D., Wang, M., Hengartner, N., Lesins, G., Dubey, M.K., 2022. Annual mean Arctic amplification 1970–2020: observed and simulated by CMIP6 climate models. *Geophys. Res. Lett.* 49 (13), 1–8. <https://doi.org/10.1029/2022GL099371>.
- Clausen, K.K., Clausen, P., 2013. Earlier Arctic springs cause phenological mismatch in long-distance migrants. *Oecologia* 173, 1101–1112.
- Conradie, S.R., Woodborne, S.M., Cunningham, S.J., McKechnie, A.E., 2019. Chronic, subtle effects of high temperatures will cause severe declines in southern African arid-zone birds during the 21st century. *Proc. Natl. Acad. Sci.* 116, 14065–14070.
- Cook, T.R., Martin, R., Roberts, J., Häkkinen, H., Botha, P., Meyer, C., Sparks, E., Underhill, L.G., Ryan, P.G., Sherley, R.B., 2020. Parenting in a warming world: thermoregulatory responses to heat stress in an endangered seabird. *Conserv. Physiol.* 8, coz109.
- Dey, C.J., Richardson, E., McGeachy, D., Iverson, S.A., Gilchrist, H.G., Semeniuk, C.A., 2017. Increasing nest predation will be insufficient to maintain polar bear body condition in the face of sea ice loss. *Global Change Biology* 23 (5), 1821–1831.
- Dobson, A., Molnár, P.K., Kutz, S., 2015. Climate change and Arctic parasites. *Trends Parasitol.* 31, 181–188.

- Dzialowski, E.M., 2005. Use of operative temperature and standard operative temperature models in thermal biology. *J. Therm. Biol.* 30 (4), 317–334.
- Elliott, K.H., Gaston, A.J., Crump, D., 2010. Sex-specific behavior by a monomorphic seabird represents risk partitioning. *Behav. Ecol.* 21, 1024–1032.
- Elmore, R.D., Carroll, J.M., Tanner, E.P., Hovick, T.J., Grisham, B.A., Fuhlendorf, S.D., Windels, S.K., 2017. Implications of the thermal environment for terrestrial wildlife management. *Wildl. Soc. Bull.* 41, 183–193.
- Frederiksen, M., Descamps, S., Erikstad, K.E., Gaston, A.J., Gilchrist, H.G., Grémillat, D., Thórarinnsson, T.L., 2016. Migration and wintering of a declining seabird, the thick-billed murre *Uria lomvia*, on an ocean basin scale: conservation implications. *Biol. Conserv.* 200, 26–35.
- Gaston, A.J., Elliott, K.H., 2013. Effects of climate-induced changes in parasitism, predation and predator-predator interactions on reproduction and survival of an Arctic marine bird. *Arctic* 43–51.
- Gaston, A.J., Hipfner, J.M., 2020. Thick-Billed Murre (*Uria lomvia*). *Birds of the World*. Cornell Lab of Ornithology, Ithaca, NY, USA.
- Gaston, A.J., Hipfner, J.M., Campbell, D., 2002. Heat and mosquitoes cause breeding failures and adult mortality in an Arctic-nesting seabird. *Ibis* 144, 185–191.
- Gilchrist, H.G., Gaston, A.J., Smith, J.N., 1998. Wind and prey nest sites as foraging constraints on an avian predator, the glaucous gull. *Ecology* 79 (7), 2403–2414.
- Grant, B.W., Dunham, A.E., 1988. Thermally imposed time constraints on the activity of the desert lizard *Sceloporus merriami*. *Ecology* 69 (1), 167–176.
- Hertz, P.E., 1992. Temperature regulation in Puerto Rican Anolis lizards: a field test using null hypotheses. *Ecology* 73 (4), 1405–1417.
- Juhasz, C.C., Shipley, B., Gauthier, G., Berteaux, D., Lecomte, N., 2020. Direct and indirect effects of regional and local climatic factors on trophic interactions in the Arctic tundra. *J. Anim. Ecol.* 89 (3), 704–715.
- Le Pogam, A., Love, O.P., Régimbald, L., Dubois, K., Hallot, F., Milbergue, M., et al., 2020. Wintering snow buntings elevate cold hardiness to extreme levels but show no changes in maintenance costs. *Physiol. Biochem. Zool.* 93, 417–433. <https://doi.org/10.1086/711370>.
- Love, O.P., Gilchrist, H.G., Descamps, S., Semeniuk, C.A., Bêty, J., 2010. Pre-laying climatic cues can time reproduction to optimally match offspring hatching and ice conditions in an Arctic marine bird. *Oecologia* 164, 277–286.
- McKechnie, A.E., Wolf, B.O., 2010. Climate change increases the likelihood of catastrophic avian mortality events during extreme heat waves. *Biol. Lett.* 6 (2), 253–256. <https://doi.org/10.1098/rsbl.2009.0702>.
- O'Connor, R., Brigham, R., McKechnie, A., 2018. Extreme operative temperatures in exposed microsites used by roosting rufous-cheeked nightjars (*Caprimulgus rufigena*): implications for water balance under current and future climate conditions. *Can. J. Zool.* 96, 1122–1129.
- O'Connor, R.S., Le Pogam, A., Young, K.G., Love, O.P., Cox, C.J., Roy, G., Robitaille, F., Elliott, K.H., Hargreaves, A.L., Choy, E.S., 2022. Warming in the land of the midnight sun: breeding birds may suffer greater heat stress at high-versus low-Arctic sites. *Proc. R. Soc. B* 289, 20220300.
- O'Connor, R.S., Love, O.P., Régimbald, L., Le Pogam, A., Gerson, A.R., Elliott, K.H., Vézina, F., 2024. An arctic breeding songbird overheats during intense activity even at low air temperatures. *Sci. Rep.* 14 (1), 15193.
- Olin, A.B., Dück, L., Berglund, P.A., Karlsson, E., Bohm, M., Olsson, O., Hentati-Sundberg, J., 2023. Breeding failures and reduced nest attendance in response to heat stress in a high-latitude seabird. *Mar. Ecol. Prog. Ser.* 737, 147–160.
- Oswald, S.A., Arnold, J.M., 2012. Direct impacts of climatic warming on heat stress in endothermic species: seabirds as bioindicators of changing thermoregulatory constraints. *Integr. Zool.* 7, 121–136.
- Patterson, A., Gaston, A.J., Eby, A., Gousy-Leblanc, M., Provencher, J.F., Braune, B.M., Elliott, K.H., 2024. Monitoring Colonial Cliff-Nesting Seabirds in the Canadian Arctic: The Coats Island Field Station. *Arctic Science*.
- Post, E., Forchhammer, M.C., Bret-Harte, M.S., Callaghan, T.V., Christensen, T.R., Elberling, B., Fox, A.D., Gilg, O., Hik, D.S., Høye, T.T., 2009. Ecological dynamics across the Arctic associated with recent climate change. *Science* 325, 1355–1358.
- R Core Team, 2022. R: A Language and Environment for Statistical Computing. R Foundation for Statistical Computing, Vienna, Austria. <http://www.R-project.org/>.
- Rantanen, M., Karpechko, A.Y., Lipponen, A., Nordling, K., Hyvärinen, O., Ruosteenoja, K., Vihma, T., Laaksonen, A., 2022. The Arctic has warmed nearly four times faster than the globe since 1979. *Commun. Earth Environ.* 3 (1), 1–10. <https://doi.org/10.1038/s43247-022-00498-3>.
- Schindelin, J., Arganda-Carreras, I., Frise, E., Kaynig, V., Longair, M., Pietzsch, T., Preibisch, S., Rueden, C., Saalfeld, S., Schmid, B., 2012. Fiji: an open-source platform for biological-image analysis. *Nat. Methods* 9, 676–682.
- Scholander, P.F., Hock, R., Walters, V., Johnson, F., Irving, L., 1950. Heat regulation in some arctic and tropical mammals and birds. *Biol. Bull.* 99, 237–258.
- Schreiber, E.A., Burger, J., 2001. *Biology of Marine Birds*. CRC Press.
- Sears, M.W., Hayes, J.P., O'Connor, C.S., Geluso, K., Sedinger, J.S., 2006. Individual variation in thermogenic capacity affects above-ground activity of high-altitude deer mice. *Funct. Ecol.* 97–104.
- Shine, R., Kearney, M., 2001. Field studies of reptile thermoregulation: how well do physical models predict operative temperatures? *Funct. Ecol.* 282–288.
- Speakman, J.R., Król, E., 2010. Maximal heat dissipation capacity and hyperthermia risk: neglected key factors in the ecology of endotherms. *J. Anim. Ecol.* 79 (4), 726–746.
- Tattersall, G., 2019. ThermImageJ: Thermal Image Functions and Macros for ImageJ. *Usamentiaga, R., Venegas, P., Guerediaga, J., Vega, L., Molleda, J., Bulnes, F.G., 2014. Infrared thermography for temperature measurement and non-destructive testing. Sensors* 14 (7), 12305–12348.
- Watson, C.M., Francis, G.R., 2015. Three dimensional printing as an effective method of producing anatomically accurate models for studies in thermal ecology. *J. Therm. Biol.* 51, 42–46.